Evolution of immune chemoreceptors into sensors of the outside world

Quentin Dietschi[a,b,1], Joël Tuberosa[a,b,1], Lone Rösingh[a,b], Gregory Loichot[a], Manuel Ruedi[c], Alan Carleton[b,d,2,3], and Ivan Rodriguez[a,b,2,3]

[a]Department of Genetics and Evolution, University of Geneva, Geneva 1205, Switzerland; [b]Geneva Neuroscience Center, University of Geneva, Geneva 1205, Switzerland; [c]Department of Mammalogy and Ornithology, Natural History Museum of Geneva, Geneva 1208, Switzerland; and [d]Department of Basic Neurosciences, School of Medicine, University of Geneva, Geneva 1205, Switzerland

Edited by Thomas C. Kaufman, Indiana University, Bloomington, IN, and approved June 2, 2017 (received for review March 10, 2017)

Changes in gene expression patterns represent an essential source of evolutionary innovation. A striking case of neofunctionalization is the acquisition of neuronal specificity by immune formyl peptide receptors (Fprs). In mammals, Fprs are expressed by immune cells, where they detect pathogenic and inflammatory chemical cues. In rodents, these receptors are also expressed by sensory neurons of the vomeronasal organ, an olfactory structure mediating innate avoidance behaviors. Here we show that two gene shuffling events led to two independent acquisitions of neuronal specificity by Fprs. The first event targeted the promoter of a V1R receptor gene. This was followed some 30 million years later by a second genomic accident targeting the promoter of a V2R gene. Finally, we show that expression of a vomeronasal Fpr can reverse back to the immune system under inflammatory conditions via the production of an intergenic transcript linking neuronal and immune Fpr genes. Thus, three hijackings of regulatory elements are sufficient to explain all aspects of the complex expression patterns acquired by a receptor family that switched from sensing pathogens inside the organism to sensing the outside world through the nose.

olfaction | vomeronasal organ | olfactory receptor | gene evolution | neofunctionalization

Genetic variability, the substrate for selective forces during evolution, relies on genetic accidents. These accidents can trigger a variety of changes, of innovations ranging from the alteration of protein identity to the modulation of transcriptional activity. In mammals, genes expressed in the olfactory system (more precisely, those coding for olfactory chemosensors) evolve very quickly, because unusual selective pressures act on this system (1–3). Thus, studying the dynamics of olfactory chemoreceptor diversity offers a unique opportunity to identify the molecular events at the origin of the genetic novelties that underlie evolutionary processes.

To extract information from an unknown outside world, mammals use a wide variety of olfactory chemosensory receptors. These receptors, most of which are G protein-coupled receptors, are expressed by neurons localized in the main olfactory neuroepithelium or in the vomeronasal organ (VNO). Based on their amino acid sequences, they are classified into various families, including the odorant receptor (Or), trace amine receptor (Taar), type A membrane-spanning four-domain protein (Ms4a), vomeronasal type 1 (V1r) and type 2 (V2r) receptor, and formyl peptide receptor (Fpr) families (1).

The olfactory sensory toolbox used by mammals is remarkable because of the extraordinary size diversity of the gene repertoires encoding it. For example, mice, humans, and elephants dispose of 1,200, 450, and 2,000 different Or genes, respectively. Similarly, the mouse and the rat genomes each contain more than 200 V1r genes, whereas the human, snake, and fish genomes harbor fewer than 10 Vrs. Moreover, the toolbox also differs from one species to another, even closely related ones, in the identity of the members pertaining to a given sensor family. This interspecies chemosensor repertoire variability reaches an extreme with the olfactory Fpr family. Indeed, Fpr olfactory expression appears to have been acquired by rodents and to be restricted to this clade, despite its expression in the immune system of all mammals. Thus, mice, rats, and gerbils express Fprs in a punctate and monogenic pattern in vomeronasal sensory neurons (4, 5), which is the singular rule characterizing the transcription of olfactory chemoreceptor genes (6).

The mouse genome contains seven Fpr genes that are expressed by immune cells, by olfactory neurons, or by both cell types. *Fpr1* and *Fpr-rs2* are transcribed by monocytes/macrophages, *Fpr-rs1* is transcribed by immune cells and vomeronasal sensory neurons, and *Fpr-rs3*, *-rs4*, *-rs6*, and *-rs7* are transcribed only by sensory neurons (4, 5). Both immune and vomeronasal Fprs recognize ligands that are linked to pathogens or to pathogenic states (4, 7, 8); what makes them different is apparently the world that they probe.

The vomeronasal sensory neuroepithelium is pseudostratified and composed of two functionally different types of neurons, organized into a basal layer and an apical layer. *Fpr-rs1* is transcribed by basal vomeronasal neurons, whereas *Fpr-rs3*, *-rs4*, *-rs6*, and *-rs7* are expressed by those located in the apical part of the neuroepithelium (4, 5). The axonal projections of like vomeronasal sensory neurons (i.e, those expressing the same chemoreceptor gene) reach the accessory olfactory bulb in the brain, where they

Significance

Immune formyl peptide receptors (Fprs) evolved in rodents from expression in immune cells to be transcribed in olfactory sensory neurons. Explaining the initial neuronal acquisition, we found that an Fpr coding exon landed in front of a vomeronasal receptor promoter, hijacking its expression pattern. This type of gene shuffling occurred twice in the mouse lineage, many million years apart, leading to the exclusive expression of Fprs in the two main populations of vomeronasal sensory neurons. Finally, we demonstrate that the immune expression of one of the mouse vomeronasal Fprs can be restored via the production of an intergenic transcript. Thus, we provide the complete history of genomic events that led to a model case of evolutionary neofunctionalization in a mammal.

Author contributions: Q.D., J.T., A.C., and I.R. designed research; Q.D., J.T., L.R., and G.L. performed research; M.R. contributed new reagents/analytic tools; Q.D., J.T., L.R., A.C., and I.R. analyzed data; and A.C. and I.R. wrote the paper.

The authors declare no conflict of interest.

This article is a PNAS Direct Submission.

Freely available online through the PNAS open access option.

Data deposition: The sequences reported in this paper have been deposited in the GenBank database (accession nos. MF175578–MF175624).

[1]Q.D. and J.T. contributed equally to this work.

[2]A.C. and I.R. contributed equally to this work.

[3]To whom correspondence may be addressed. Email: alan.carleton@unige.ch or ivan.rodriguez@unige.ch.

This article contains supporting information online at www.pnas.org/lookup/suppl/doi:10.1073/pnas.1704009114/-/DCSupplemental.

coalesce and form multiple structures called glomeruli. This is true for V1rs (9, 10), V2rs (11), and Fprs (12). Vomeronasal sensory neurons located in the apical and basal zones do recognize different types of chemicals, mainly kairomones (semiochemicals that mediate interspecific interactions). Activation of these neuronal populations often leads to innate and stereotyped behaviors (13–15).

In this study, we show that two independent exon shufflings associated with the production of an intergenic splice variant explain how, starting from an immune specificity, Fprs acquired their complex expression patterns in neurons during evolution.

Results and Discussion

The Different Identities of Olfactory and Immune Fprs. Patterns of Fpr expression are complex. In the mouse, *Fpr1* and *Fpr-rs2* are transcribed by monocytes/macrophages, *Fpr-rs1* is transcribed by immune cells and basal vomeronasal sensory neurons, and *Fpr-rs3*, *-rs4*, *-rs6*, and *-rs7* transcripts are found only in apical vomeronasal sensory neurons (4, 5, 16) (Fig. 1*A*). To study the evolutionary history of the Fpr repertoires, we performed homology searches across genome assemblies of 32 mammalian species, from which we retrieved 101 Fpr coding sequences. In addition, we harvested tissue samples from 15 Eumuroida species and identified 39 new Fpr sequences with a degenerate PCR approach. The resulting Fpr gene phylogeny demonstrates the massive diversification of the repertoires (Fig. 1*A*). Supporting the peculiar dynamics of the Fpr family, a synteny analysis of the Fpr cluster between the rat and the mouse shows high rates of gene birth and death (Fig. S1 *A* and *B*).

To determine the time at which Fprs first acquired neuronal expression, we tested multiple species for vomeronasal and immune Fpr expression. In most Eumuroida species tested (a group representing 23% of mammalian species living today), we found at least one Fpr gene transcribed in vomeronasal sensory neurons, and none outside of this rodent family (Fig. 1 *A* and *D* and Fig. S2). Analysis of the tree thus suggests that the split between immune and apical vomeronasal Fprs occurred at the root of the Eumuroida group, and that *Fpr-rs3* (which is present across the Eumuroida lineage, whereas the *Fpr-rs4*, *-rs7*, and *-rs6* orthologs are found only in the Murinae group), corresponds to the first vomeronasal Fpr (Fig. 1*A*).

Neofunctionalization of vomeronasal Fprs is associated with the development of specific agonist properties (4, 7, 8) and signatures of positive selection (5). To investigate protein characteristics that could have been acquired by vomeronasal Fprs, we analyzed the sequence of FPR-rs3 in 17 rodent species. We identified 10 amino acids that were fixed in FPR-rs3 of all tested species and that were always absent from immune Fprs (Fig. 1*B* and Fig. S3). The position of one of these differentially conserved amino acids (His106) was previously identified by modeling approaches as likely having a role in ligand recognition by Fprs (17). To evaluate the selective pressures acting on the immune and the vomeronasal Fprs, we then calculated pairwise K_a/K_s ratios [the rate of nonsynonymous substitutions (K_a) over the rate of synonymous substitutions (K_s)] for *Fpr-rs3*, *Fpr-rs2*, and *Fpr1* of the different rodent species. The ratios show that both immune and vomeronasal Fprs are under purifying selection. They also indicate lower values when comparing *Fpr1* and *Fpr-rs2* sequences than when comparing *Fpr1* and *Fpr-rs3* sequences (Fig. 1*C*).

Across species, Fpr genes are consistently grouped in the genome and neighbor a cluster of vomeronasal receptor genes (Fig. 1*D* and Fig. S1*C*). In non-Eumuroida species, a split between Fprs on one side and the Vr gene cluster composed of V1rs but lacking V2rs on the other side is observed, with no intermingling (Fig. 1*D* and Fig. S1*C*). In contrast, in the Eumuroida group (18), multiple Fprs are also embedded inside the Vr cluster that contains both V1rs and V2rs. It is these Fprs, located outside of the ancestral immune Fpr cluster, that are expressed in VSNs (Fig. 1 *A* and *D*). Thus, the physical proximity of Fprs with Vrs (and therefore with their regulatory elements) is correlated both with the arrival of V2rs in the Fpr/Vr cluster and with the acquisition of neuronal specificity, suggesting a causative link between Fpr/Vr intermingling and vomeronasal expression.

Fpr Promoters Driving Apical Vomeronasal Neuron Expression Were Initially V1r Gene Promoters. To identify the genomic events that led to the acquisition of vomeronasal specificity by Fpr genes, we analyzed the genomic elements that potentially control their expression. We initially focused our attention on the *Fpr-rs3* gene, because it is conserved among Eumuroida and thus can be used for interspecies comparisons (Fig. 1*A*). We divided the sequence of *Fpr-rs3* into three regions: the *Fpr-rs3* promoter, the *Fpr-rs3* first and noncoding exon, and the *Fpr-rs3* coding sequence. Homologies with these sequences were searched in the mouse, rat, rabbit, guinea pig, horse, and cat genomes. High sequence homologies (up to 90% identity) were found between the *Fpr-rs3* promoter and all promoters of Fpr genes transcribed in the apical layer of the VNO (Fig. 2*A*). No homology was found with the promoters of *Fpr-rs1* (expressed in basal vomeronasal neurons) and with the two immune Fpr genes. Interestingly, we found high sequence homologies (59–70%) of the promoter and the first noncoding exon of *Fpr-rs3* with V1r genes of the rabbit, guinea pig, horse, and cat (Fig. 2*A*), whereas only vomeronasal Fpr sequences were matched in the mouse. This suggests that the gene shuffling event had led to the hijacking of a V1r regulatory sequence, with the functional elimination of its coding sequence (CDS) as a side effect. This was confirmed by the identification of V1r CDS remnants between the first noncoding exons of vomeronasal Fpr genes and their CDSs, which we identified in the mouse and rat genomes (Fig. 2 *A–D* and Fig. S4 *A* and *B*). A V1r phylogeny found that these remnants correspond to a V1r family (which we term V1rx) that disappeared in Eumuroida following the exon shuffling (Fig. S4*C*). Taken together, these findings indicate that an exon shuffling event involving the last and coding exon of an immune Fpr gene (a gene more closely related to *Fpr-rs2* than to *Fpr1* based on phylogenetic analyses) targeted a V1r gene in a rodent living between 31 and 71 Mya (19). This provided a novelty to the rodent chemosensory toolbox, an innovation that has been expanded and maintained until today.

The Fpr Promoter Driving Basal Vomeronasal Neuron Expression Was Initally a V2r Gene Promoter. In the mouse VNO, *Fpr-rs1* is transcribed exclusively in basal vomeronasal neurons (4, 5). Because V2rs are expressed in the basal part of the vomeronasal epithelium, unlike V1rs, we wondered whether a similar type of genomic accident—that is, an exon shuffling but this time involving a V2r gene—could be at the origin of this novel Fpr transcription pattern. We found significant sequence homologies (up to 75%) between the mouse *Fpr-rs1* promoter or its first noncoding exon and mouse V2r promoters (Fig. 2*E*). We observed a complete lack of homology between the *Fpr-rs1* CDS and the V2R CDSs and an 81.5% identity with the one of the immune *Fpr-rs2* (Fig. 2*E*). This Fpr expression in the basal vomeronasal zone likely represents a recent acquisition that postdates the split between rats and mice, given that we found no sequence homologies between Fpr promoters and V2r promoters in the rat, hamster, or guinea pig. Moreover, we did not find *Fpr-rs1* in *Apodemus sylvaticus*, suggesting that the acquisition is restricted to the *Mus* genus.

The acquisition of Fpr expression by both apical and basal vomeronasal sensory neurons is not just more of the same, because although these two types of sensory neurons mediate the perception of pheromones and kairomones, they are not equivalent. They each project to well-defined and distinct parts of the accessory olfactory bulb (9, 10), a segregation maintained at the level of the projections of the corresponding secondary neurons

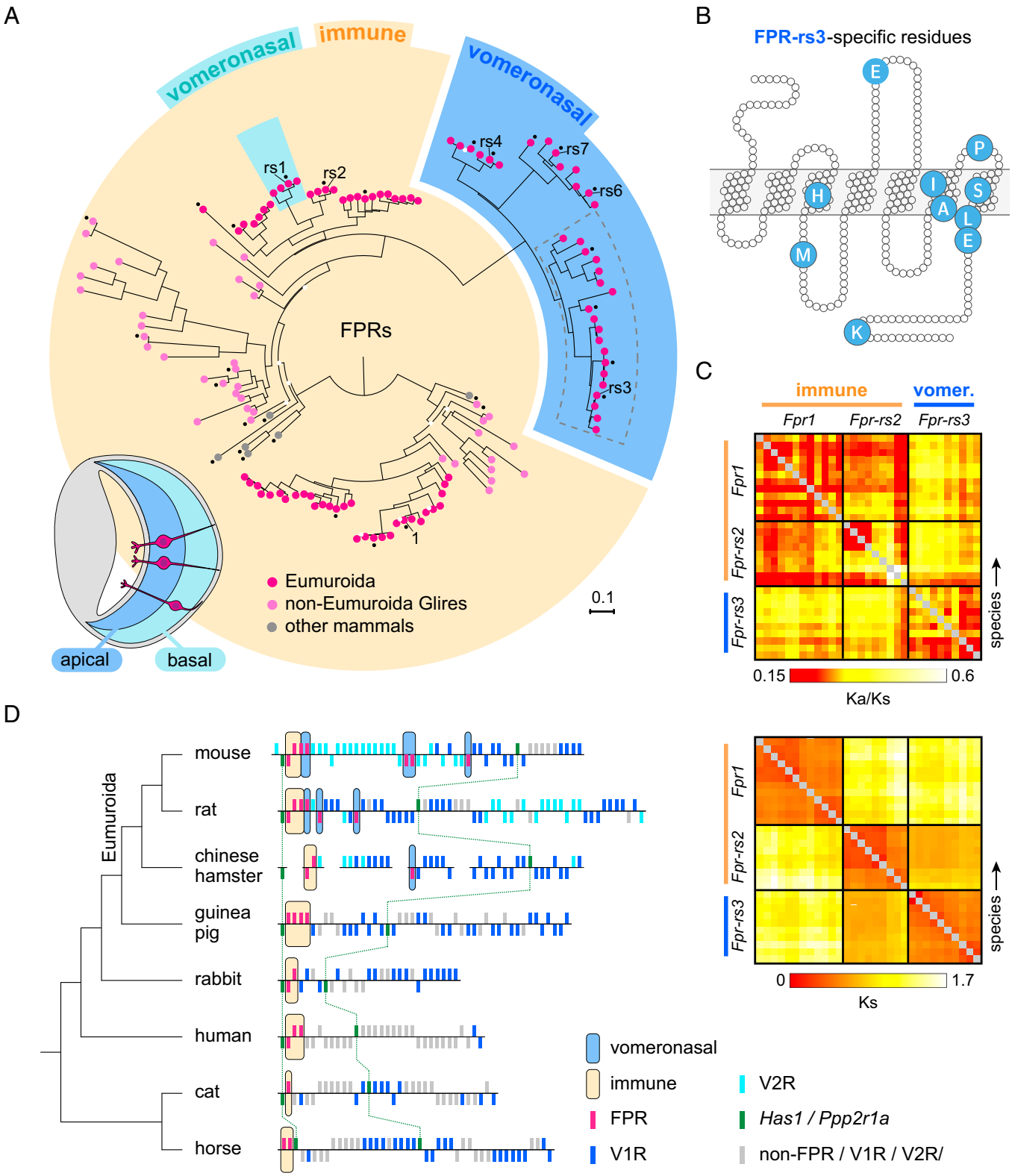

Fig. 1. The different identities of olfactory and immune Fprs. (*A*) Phylogenetic relationships between Fprs pertaining to 32 different mammalian species (16 Eumuroida, 12 non-Eumuroida glires, and 4 other mammals). The tree was inferred from a protein alignment with a maximum likelihood approach. The scale bar corresponds, for each branch, to amino acid substitutions per site. Branches with low bootstrap support (<30%) are indicated by a white disk. Black dots indicate species for which Fpr tissue specificity (vomeronasal or immune) was evaluated by qPCR, RNA-seq, or immunohistochemistry. On the bottom left part of the tree, the schematic represents a coronal section through a VNO with its basal and apical neuroepithelium. The dotted area encompasses all FPR-rs3 orthologs. (*B*) Conserved amino acid residues present in FPR-rs3 of all tested species and never observed in FPR-rs2 or FPR1. Colored residues are conserved at 100% in FPR-rs3 of all tested rodent species (n = 17 species, 18 alleles) (Fig. S3). (*C*) Pairwise K_a/K_s ratios and K_s rates of immune and vomeronasal Fprs from various rodent species (the row order follows the order in Fig. S3). (*D*) Intermingling between Fpr and Vr genes is associated with vomeronasal Fpr expression. As landmarks of the synteny, the *Has1* and *Ppp2r1a* nonolfactory genes are shown in green. Genomic coordinates are indicated in Table S6. Genes (colored rectangles) are arranged according to their transcriptional orientation.

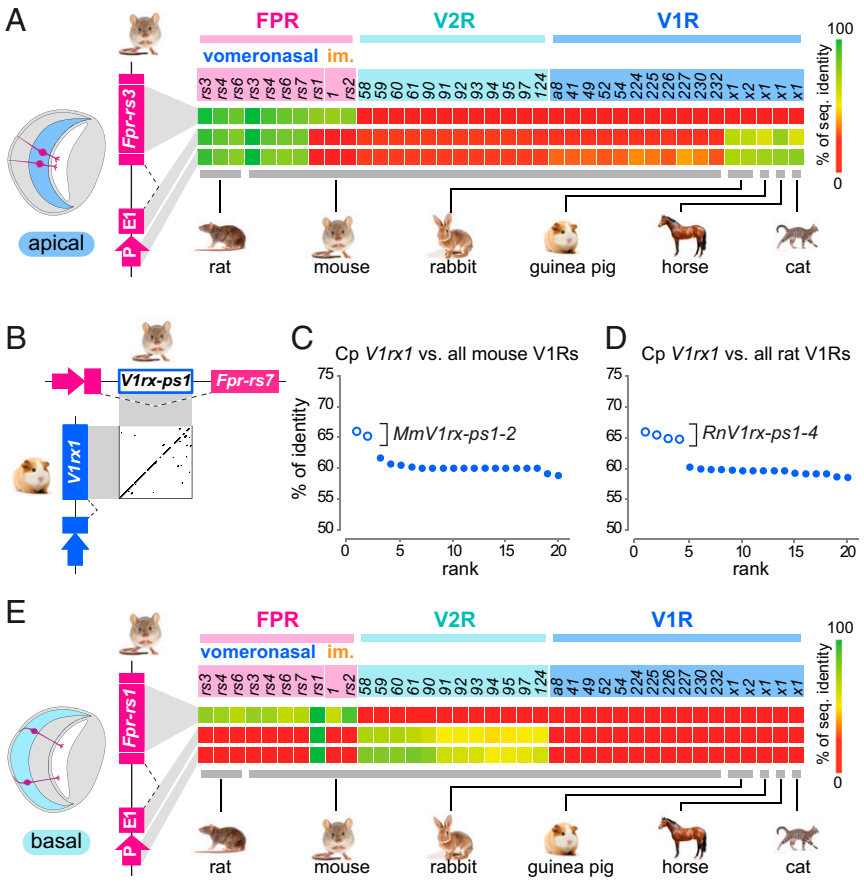

Fig. 2. Fpr promoters driving apical and basal vomeronasal neuron expression were originally V1r and V2r promoters, respectively. (*A*) Sequence identities between the mouse *Fpr-rs3* promoter and first noncoding exon, and the corresponding segments of Fpr, V1r, and V2r genes from various species are shown. Homologies corresponding to the CDS are amino acid identities. The blue color in the vomeronasal schematic indicates the apical layer in which *Fpr-rs3*, *Fpr-rs4*, *Fpr-rs6*, and *Fpr-rs7* are transcribed. (*B*) Blast2 plots showing homologies (the dotted transverse line) between *CpV1rx1* and pseudogenic remnants of V1r coding sequences located between exon 1 and the coding sequence of the mouse *Fpr-rs7*. (*C* and *D*) Closest relatives to *CpV1rx* in the mouse genome (*V1rx-ps1* and *V1rx-ps2*) and in the rat genome (*RnV1rx-ps1*, *RnV1rx-ps2*, *RnV1rx-ps3*, and *RnV1rx-ps4*). (*E*) Sequence identities as in *A*, but with the basally expressed *Fpr-rs1*.

(20). Moreover, functionally, the silencing of either apical or basal vomeronasal sensory neurons in the mouse leads to different phenotypes (21, 22). Thus, it appears that in terms of mechanism, similar to what was observed for the acquisition of Fpr transcriptional activity in apical vomeronasal sensory neurons (but later during evolution), a copy of the *Fpr-rs2* CDS landed just after the first exon of a V2r gene. It benefited from its regulatory elements, and provided a completely novel tool for a sensory population involved in perceiving the outside world.

Reacquisition of Immune Specificity by *Fpr-rs1*. Despite the acquisition of neuronal tissue specificity by *Fpr-rs1*, this gene remains expressed in cells of the immune system under specific conditions, particularly after an inflammatory challenge with lipopolysaccharide (LPS), similar to immune Fpr genes (16, 23, 24) (Fig. 3*A*). To explain this conditional switch, we considered that a de novo acquisition of immune specificity by the *Fpr-rs1* promoter was unlikely to have followed exon shuffling. Therefore, we looked for an alternative explanation and investigated the potential hijacking by the splice acceptor site of the CDS-containing *Fpr-rs1* exon of a splice donor site from another gene transcribed in immune cells. We found that an *Fpr-rs1* chimeric mRNA is produced by bone marrow cells after LPS exposure (Fig. 3 *A* and *B*). Its synthesis is driven in *cis* by the promoter of the immune *Fpr-rs2*, which is located 83 kb upstream of *Fpr-rs1* and in the same transcriptional orientation. This chimeric transcript is composed on its 5′ end of the first noncoding exon of *Fpr-rs2*, followed by a short *Fpr-rs1* 5′UTR, and by the *Fpr-rs1* CDS. Unlike what is observed for V1r genes, the first exon of V2r genes is coding, leading in our case to the potential production of a chimeric protein (an Fpr with an extracellular V2r N terminus), because both the V2r and the Fpr CDSs are in frame. However, no such chimeric protein is produced, because a stop codon is generated at the splice site between the V2r first exon and the Fpr exon containing the CDS. Thus, the dual neural and immune expression pattern acquired by *Fpr-rs1* is achieved by a double mechanism, with each mechanism taking advantage of a different promoter.

Conclusion

We have provided evidence that in the rodent lineage, an exon shuffling event first led to the expression of Fprs in apical vomeronasal neurons. More than 15 million y later, in the *Mus* lineage, this was followed by another exon shuffling event that drove the transcription of an Fpr gene in basal vomeronasal neurons, and a context-dependent intergenic splice that maintained an immune specificity to this latter Fpr (Fig. S5 and Movie S1). The functional integration of Fprs into the VNO was likely favored by the versatility of the recipient system and by the dual role played by vomeronasal chemoreceptors. Indeed, vomeronasal receptors not only sense the outside world, but also play a critical role in the wiring of the system. When the coding sequence of a V1r receptor gene is deleted, axonal fibers from

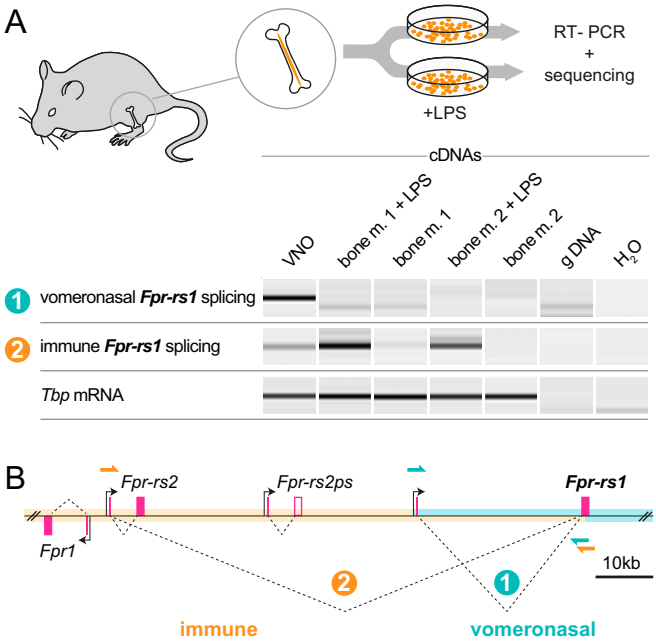

Fig. 3. Reacquisition of immune specificity by *Fpr-rs1*. (*A*, *Upper*) Schematic representing the experimental design. (*A*, *Lower*) RT-PCR (primer locations indicated in *B*) showing two *Fpr-rs1* transcript variants, one driven by the *Fpr-rs1* promoter and the other driven by the immune *Fpr-rs2* promoter. The abundance of this latter intergenic splice variant increases in bone marrow cells after LPS treatment. (*B*) Schematic corresponding to the vomeronasal (1) and immune (2) *Fpr-rs1* transcripts.

neurons expressing this mutant allele lose their ability to coalesce and to form glomeruli in the accessory olfactory bulb; however, when this V1r coding sequence is swapped with the one of an Or (Ors share no sequence homologies with V1rs), vomeronasal axons regain the ability to form glomeruli (9). Thus, a few simple and specific hijackings of regulatory elements were sufficient to provide an entire mammalian clade with a completely novel sensory toolbox to extract information from the outside world.

Methods

Identification of Chemosensory Receptor Gene Repertoires. The whole mouse gene repertoires encoding V1rs, V2rs, and Fprs were retrieved from the mouse genome assembly GRCm38/mm10 using the Ensembl Biomart interface and filtering for InterPro signatures IPR004072 (vomeronasal receptor type 1), IPR004073 (vomeronasal receptor type 2), and IPR000826 (formyl peptide receptor-related) (25). The corresponding protein sequences were used to identify each species repertoire (Table S1) with tblastn searches (e-value < 1e-20). ORFs with fewer than seven TMHMM-predicted (26) transmembrane domains were discarded. For each repertoire, a neighbor-joining tree was built using closely related protein families as outgroups (T2rs for V1rs, T1rs and *Casr* for V2rs, and *GPR32* for Fprs). Genes branching with the outgroup were filtered out. For Fpr gene identification in nonsequenced rodent species, rodent tissue samples were taken from our own collection (*Mesocricetus auratus*, *Phodopus roborovskii*, *Acomys dimidiatus*, *Meriones unguiculatus*, and *Phodopus sungorus*) and from the Natural History Museum of Geneva (*Rattus exulans*, *Rattus rattus*, *Niviventer langbianis*, *Microtus regalis*, *Microtus arvalis*, *Apodemus alpicola*, *Apodemus flavicollis*, *A. sylvaticus*, and *Micromys minutus*). DNAs were extracted, and homologs of mouse *Fpr1*, *Fpr-rs2*, and *Fpr-rs3* were amplified by PCR with degenerate primers located on ortholog-specific conserved sequence segments (Table S2). All sequences are available in Dataset S1, and those absent from genome databases were submitted to GenBank (accession nos. MF175578–MF175624).

Gene Phylogenies. Multiple sequence alignments were performed with the MAFFT aligner program using the G-INS-i setting (27). Because V2r subfamilies have nonhomologous exons, we kept the alignable part of the proteins and trimmed their alignment before the PxSxC[ST]xxC motif (located upstream of the first transmembrane domain) and after the end of the last transmembrane domain. For all alignments, columns containing >90% gaps were discarded from the phylogenetic analysis. Protein duplicates corresponding to silent polymorphic variants were discarded as well. ProtTest 3 (28) was then used to determine the best-fitting model of evolution to build the trees. Maximum likelihood phylogenies were calculated using PhyML 3 (29). Branch supports were assessed using the nonparametric Shimodaira–Hasegawa-like approximated likelihood ratio test and, for the Fpr phylogeny, also by 1,000 bootstrap replicates. Subsequent phylogenies were used to establish the Fpr, V1r, and V2r gene syntenies in the Fpr/Vr gene cluster between the mouse and the rat. We adapted our species tree to the phylogeny published by Fabre et al. (30).

Transcription Start Site Identification. To determine *Mus musculus Fpr-rs1* and *Fpr-rs3* transcription start sites (TSSs), their first noncoding exons were identified by assembling RNA sequencing (RNA-seq) reads from whole VNOs. The assembled transcripts were then blasted against the mouse genome (GRCm38/mm10) to define their coordinates.

Promoters, First Exons, and CDS Comparisons. Sequences upstream from TSSs and first exons from mouse *Fpr-rs1* and *Fpr-rs3* were used as blastn queries in genomes from different species to retrieve sequences that share similarities. These sequences constituted a dataset to which first exon sequences and sequences upstream of previously identified V1r and V2r TSSs (31) were added. Promoters, first exons, and CDSs were aligned with MAFFT using the E-INS-i setting. They were trimmed manually and curated with G-blocks (32) before the identity matrix analyses. Promoter and first exon sequence identity matrices were built with nucleotide sequences, whereas the CDS matrix identity was built with amino acid sequences. Genomic coordinates of these sequences are provided in Table S3.

Gene Expression Analyses. Before tissue extraction, animals were flushed of blood under anesthesia. Bone marrow was taken from femur, tibia, and humerus. mRNA samples were DNase-treated, and cDNAs were synthesized with random hexamers and poly-T oligonucleotides (PrimeScript RT Reagent Kit; TaKaRa). Room temperature controls were performed for all cDNAs. Quantitative PCR (qPCR) reactions were performed in triplicate in 384-well plates. SDS 2.2.1 software was used to analyze data, with a detection threshold at $\Delta Rn = 0.3$. An in-house spreadsheet was used to analyze and convert Ct values to relative values. Outliers with $\Delta Ct > 0.5$ relative to the median within a given technical triplicates were discarded. The geNorm algorithm was used to analyze the variance of the normalization genes and select them. Normalization genes and V1r- and Fpr-specific primers are listed in Table S4. For the species for which mRNA samples were disposed of, we blasted Fpr sequences on publicly available bone marrow RNA-seq reads (rabbit, SRX110712; cat, SRX1610312; horse, SRX752839, SRX752840, SRX752841, SRX752842, and SRX752843). For RNA-seq, RNAs were ribodepleted, and 100-bp reads were sequenced with the Illumina HiSeq 2500 system.

Amino Acid Conservation. To identify FPR-rs3–specific sites, we used an alignment including all identified FPR1, FPR-rs2, and FPR-rs3 sequences from Eumuroida species. FPR-rs1 sequences from *Mus* species were discarded because they are supposed to be expressed in both the immune and the vomeronasal system. FPR-rs3–specific sites were identified as being 100% conserved among all FPR-rs3 and absent in FPR1 or FPR-rs2 at homologous positions. For K_a/K_s estimations, the alignment of codons was inferred from the protein alignment. We then selected a subset of sequences separated with a minimum evolutionary distance ($K_s \geq 0.1$). Positions with gaps were removed, and estimated K_a/K_s ratios were computed for all pairs using the pairwise mode of codeml in the PAML 4.9c package (33) (runmode = −2, CodonFreq = 0, fix_kappa = 1).

***Fpr-rs1* Expression.** Bone marrow was flushed from mouse femurs and tibias. Bone marrow cells were resuspended at 4×10^6 cells/mL, plated at 1×10^7 cells per 60-mm dish, and left for 2 h at 37 °C. PBS or PBS + 150 μg/mL of LPS (*Salmonella* enteriditis) was added to the cultures, which were then maintained at for 8 h at 37 °C. mRNAs were extracted and reverse-transcribed. PCR conditions are specified in Table S5. All PCR amplicons were sequenced.

ACKNOWLEDGMENTS. We thank Benoît von der Weid, Francisco Resende, Chenda Kan, and Véronique Jungo for expert technical help, and thank the Milinkovitch laboratory for *Acomys dimidiatus* genomic DNA. This work was supported by the Claraz Foundation, and the Swiss National Science Foundation Grants 31003A_170114 (to I.R.), CR33I3_143723 (to I.R. and A.C.), and 31003A_172878 (to A.C.).

1. Bear DM, Lassance J-M, Hoekstra HE, Datta SR (2016) The evolving neural and genetic architecture of vertebrate olfaction. *Curr Biol* 26:R1039–R1049.
2. Niimura Y, Nei M (2006) Evolutionary dynamics of olfactory and other chemosensory receptor genes in vertebrates. *J Hum Genet* 51:505–517.
3. Jiang Y, Matsunami H (2015) Mammalian odorant receptors: Functional evolution and variation. *Curr Opin Neurobiol* 34:54–60.
4. Rivière S, Challet L, Fluegge D, Spehr M, Rodriguez I (2009) Formyl peptide receptor-like proteins are a novel family of vomeronasal chemosensors. *Nature* 459:574–577.
5. Liberles SD, et al. (2009) Formyl peptide receptors are candidate chemosensory receptors in the vomeronasal organ. *Proc Natl Acad Sci USA* 106:9842–9847.
6. Dalton RP, Lomvardas S (2015) Chemosensory receptor specificity and regulation. *Annu Rev Neurosci* 38:331–349.
7. Bufe B, et al. (2015) Recognition of bacterial signal peptides by mammalian formyl peptide receptors: A new mechanism for sensing pathogens. *J Biol Chem* 290:7369–7387.
8. Bufe B, Schumann T, Zufall F (2012) Formyl peptide receptors from immune and vomeronasal system exhibit distinct agonist properties. *J Biol Chem* 287:33644–33655.
9. Rodriguez I, Feinstein P, Mombaerts P (1999) Variable patterns of axonal projections of sensory neurons in the mouse vomeronasal system. *Cell* 97:199–208.
10. Belluscio L, Koentges G, Axel R, Dulac C (1999) A map of pheromone receptor activation in the mammalian brain. *Cell* 97:209–220.
11. Del Punta K, Puche A, Adams NC, Rodriguez I, Mombaerts P (2002) A divergent pattern of sensory axonal projections is rendered convergent by second-order neurons in the accessory olfactory bulb. *Neuron* 35:1057–1066.
12. Dietschi Q, Assens A, Challet L, Carleton A, Rodriguez I (2013) Convergence of FPR-rs3-expressing neurons in the mouse accessory olfactory bulb. *Mol Cell Neurosci* 56: 140–147.
13. Liberles SD (2014) Mammalian pheromones. *Annu Rev Physiol* 76:151–175.
14. Chamero P, Leinders-Zufall T, Zufall F (2012) From genes to social communication: Molecular sensing by the vomeronasal organ. *Trends Neurosci* 35:597–606.
15. Stowers L, Kuo T-H (2015) Mammalian pheromones: Emerging properties and mechanisms of detection. *Curr Opin Neurobiol* 34:103–109.
16. Stempel H, et al. (2016) Strain-specific loss of formyl peptide receptor 3 in the murine vomeronasal and immune systems. *J Biol Chem* 291:9762–9775.
17. He H-Q, Troksa EL, Caltabiano G, Pardo L, Ye RD (2014) Structural determinants for the interaction of formyl peptide receptor 2 with peptide ligands. *J Biol Chem* 289: 2295–2306.
18. Steppan S, Adkins R, Anderson J (2004) Phylogeny and divergence-date estimates of rapid radiations in muroid rodents based on multiple nuclear genes. *Syst Biol* 53: 533–553.
19. Fang X, et al. (2014) Genome-wide adaptive complexes to underground stresses in blind mole rats *Spalax*. *Nat Commun* 5:3966.
20. Mohedano-Moriano A, et al. (2007) Segregated pathways to the vomeronasal amygdala: Differential projections from the anterior and posterior divisions of the accessory olfactory bulb. *Eur J Neurosci* 25:2065–2080.
21. Norlin EM, Gussing F, Berghard A (2003) Vomeronasal phenotype and behavioral alterations in Gαi2 mutant mice. *Curr Biol* 13:1214–1219.
22. Chamero P, et al. (2011) G protein Gαo is essential for vomeronasal function and aggressive behavior in mice. *Proc Natl Acad Sci USA* 108:12898–12903.
23. Cui Y-H, et al. (2002) Bacterial lipopolysaccharide selectively up-regulates the function of the chemotactic peptide receptor formyl peptide receptor 2 in murine microglial cells. *J Immunol* 168:434–442.
24. Mandal P, Novotny M, Hamilton TA (2005) Lipopolysaccharide induces formyl peptide receptor 1 gene expression in macrophages and neutrophils via transcriptional and posttranscriptional mechanisms. *J Immunol* 175:6085–6091.
25. Mitchell A, et al. (2015) The InterPro protein families database: The classification resource after 15 years. *Nucleic Acids Res* 43:D213–D221.
26. Krogh A, Larsson B, von Heijne G, Sonnhammer EL (2001) Predicting transmembrane protein topology with a hidden Markov model: Application to complete genomes. *J Mol Biol* 305:567–580.
27. Katoh K, Standley DM (2013) MAFFT multiple sequence alignment software version 7: Improvements in performance and usability. *Mol Biol Evol* 30:772–780.
28. Darriba D, Taboada GL, Doallo R, Posada D (2011) ProtTest 3: Fast selection of best-fit models of protein evolution. *Bioinformatics* 27:1164–1165.
29. Guindon S, et al. (2010) New algorithms and methods to estimate maximum-likelihood phylogenies: Assessing the performance of PhyML 3.0. *Syst Biol* 59:307–321.
30. Fabre P-H, Hautier L, Dimitrov D, Douzery EJP (2012) A glimpse on the pattern of rodent diversification: A phylogenetic approach. *BMC Evol Biol* 12:88.
31. Ibarra-Soria X, Levitin MO, Saraiva LR, Logan DW (2014) The olfactory transcriptomes of mice. *PLoS Genet* 10:e1004593.
32. Talavera G, Castresana J (2007) Improvement of phylogenies after removing divergent and ambiguously aligned blocks from protein sequence alignments. *Syst Biol* 56:564–577.
33. Yang Z (2007) PAML 4: Phylogenetic analysis by maximum likelihood. *Mol Biol Evol* 24:1586–1591.